Proc. of the Eighth Intl. Conf. on Advances in Civil, Structural and Mechanical Engineering - CSM 2019

ISBN: 978-1-63248-170-2 DOI : 10.15224/978-1-63248-170-2-15

Behavior of Eccentric Vertical Loaded Circular Footng on Sand Layer of Limited Thickness using Finite Element

[Barada Prasad Sethy and Chittaranjan Patra]

***Abstract*—Numerical study has been carried out to determine the ultimate bearing capacity of circular footing on a sand layer of limited thickness underlain by a rigid rough base subjected to an eccentric vertical load. The sand layer for the numerical study was prepared at a relative density (*Dr*) of 69% using five different thicknesses, *H*. FE model was performed at *H*/*B* values of 0.3, 0.5, 1, 2, and 3 (*B* = diameter of footing). The load eccentricity ratio *e*/*B* varied from 0 to 0.15. The analysis was performed using an elasto-plastic hyperbolic model called the hardening soil (HS) model. Effect of the depth of rough rigid base and load eccentricity on bearing capacity was studied under eccentric vertical loading. Further, the failure mechanism under eccentric vertical loading has been studied. Numerical modeling results indicate that the bearing capacity and the depth of failure surface get modified when the rigid rough base is located at a shallow depth ($H/B \leq H/B_{cr}$) from the base of the foundation. The bearing capacity values obtained from the FE analysis are compared with the laboratory model test results.**

Keywords—circular footing, sand, rigid rough base, eccentric loading, ultimate bearing capacity, finite element

I. Introduction

Recently, an exponential development in the area of digital computers and computational mechanics has resulted in the application of the finite element method (FEM) to almost all areas of geotechnical engineering including shallow footings. The finite element method has also become a highly useful tool, and has been widely used for the numerical analysis by various authors, e.g., Bousherian and Hataf [1]; Laman and Yildiz [2]; Loukidis and Salgado [3]; Ornek et al. [4]; Kaya and Ornek [5]; Demir et al. [6]; Van Baars [7]; Yang et al. [8].

Barada Prasad Sethy
National Institute of Technology Rourkela
India

Chittaranjan Patra
National Institute of Technology Rourkela
India

In this study numerical investigations have been performed to determine the mechanical behavior, failure mechanism and the ultimate bearing capacity of circular footing on sand layer of limited thickness underlain by a rigid rough base under eccentric load (Fig. 1).

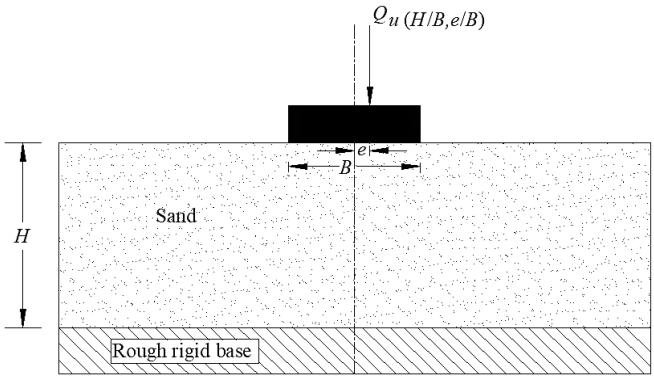

Figure 1. Shallow circular foundation on sand layer of limited thickness subjected to eccentric load (Note: *B* = diameter of the foundation, *e* = eccentricity, *H* = thickness of sand layer)

II. Finite Element Analysis

Numerical analysis is a powerful mathematical tool that makes it possible to solve complex engineering problems. The finite-element method (FEM) is a well-established numerical analysis technique used widely in many civil engineering applications, both for research and the design of real engineering problems. The constitutive behavior of soils can be successfully modeled with numerical analysis. The finite-element method is one of the mathematical methods in which continuous media is divided into finite elements with different geometries. It provides the advantages of idealizing the material behavior of soil, which is non-linear with plastic deformations and stress-path dependent, in a more rational manner. The finite element method can also be useful for identifying the deformation patterns and stress distribution in and around the soil element during deformation and at the ultimate state. The analysis was performed using finite element program Plaxis 3D by Brinkgreve and Vermeer [9]. It is a finite element package specially developed for the analysis of deformation and stability in geotechnical problems such as tunnels, deep excavations, and earth structures such as retaining walls and slopes.

Plaxis incorporates a fully automatic mesh generation process in which the geometry is divided into elements and

Proc. of the Eighth Intl. Conf. on Advances in Civil, Structural and Mechanical Engineering - CSM 2019

ISBN: 978-1-63248-170-2 DOI : 10.15224/978-1-63248-170-2-15

compatible with structural elements. Five different mesh densities are available in Plaxis ranging from very coarse to very fine. In order to obtain the most suitable mesh for the present study, preliminary computations using the five available levels of global-mesh coarseness were conducted. In the sensitivity analysis, the number of elements was changed from 5240 to 205230 (i.e. very coarse to very fine) for the axisymmetric condition as shown in Fig. 2. Figure 2 shows the mesh size which is having the minimum effect on the results after about 85000 to 170000 elements.

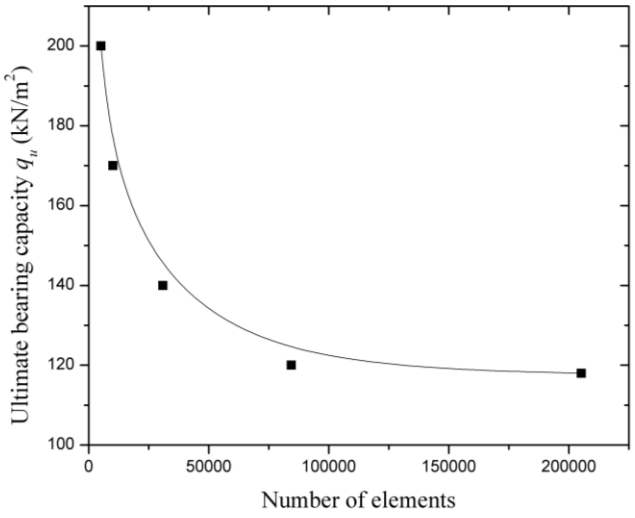

Figure 2. Influence of mesh size on the finite-element results

sand layer)

III. Finite Element Modeling

A series of HS model has been used to verify the laboratory model tests results and to understand the deformation trends within the soil mass. HS model is an advanced soil model for simulating the behavior of different types of soil both stiff soils and soft soils [10]. The nonlinear behavior of sand was modeled using HS model, which is an elastoplastic hyperbolic stress-strain model, formulated in the context of friction hardening plasticity. A basic feature of hyperbolic model is the stress dependency of soil stiffness. The HS model is formulated in the framework of the classical theory of plasticity and supersedes the hyperbolic model: first by using the theory of plasticity rather than the theory of elasticity, second by including soil dilatancy, and third by introducing a yield cap. The HS model parameters used in the FE analysis are presented in Table 1.

The model footing is assumed to rest on a sandy soil. To eliminate the boundary effect due to loading the horizontal distance was taken as three and half times the width of the footing in both the direction. The geometry of the model footing used for numerical analysis is the same as used in the laboratory model tests. The sand was modeled with suitable plan dimensions and the depth was modeled using borehole option. Soil volume elements were modeled as a 10-noded tetrahedral element and the footing was modeled as 6-noded triangular plate element. The linear elastic model was considered for the plate element with the node-to-node anchor. The drained condition is assumed for soil and non-porous for plate element. The refined mesh was adopted to minimize the effect of mesh dependency on the finite element modeling. An incremental load was applied to the footing surface. The loading point of the soil model is selected for the analysis. An important feature of this calculation procedure is that the user specifies the values of the total load to be applied. The calculations are done until the failure of the soil occurs. The load-settlement curve thus obtained from the output gave the ultimate inclined load per unit area and ultimate settlement of the circular footing by using break-point method for different loading conditions.

Table 1 HS model parameters used in the finite-element analysis

Parameter	Sand	Footing	Plate
Unit weight, γ (kN/m^3)	14.36	78.5	78.5
Triaxial loading stiffness, E_{50}^{ref} (MN/m^2)	42	2×10^5	2.1×10^5
Triaxial unloading stiffness, E_{ur}^{ref} (MN/m^2)	126	-	-
Oedometer loading stiffness, E_{oed}^{ref} (MN/m^2)	42	-	-
Soil friction angle, ϕ (°)	40.9	-	-
Poisson's ratio, ν	0.3	0.3	0.3
Dilatancy angle, ψ (°)	10.9	-	-
Reference stress for stiffness, P^{ref} (kN/m^2)	100	-	-

IV. Result and Analysis

A. *Comparison of Load Settlement Curves*

A total of 24 FE models were performed using a model circular footing. FE study on the effect of rough rigid base on load eccentricity was carried out using Plaxis 3D. A typical graded finite element mesh composed of soil, footing, and rigid rough base together with boundary conditions used. The ultimate eccentric load per unit area $q_{u\ (H/B,\ e/B)}$ for the footing-soil system are determined from the load-displacement curves as the pronounce peak after which the footing collapses and the load decreases. In curves, which did not show a definite failure point, the ultimate load is taken as the point at which the slope of the load-displacement curve first reaches to 0 or a steady minimum value (Vesic [11]). Ultimate load per unit area values for the footing on the sand layer with the rigid base at a limited depth and sand layer with the rigid base at a great depth (H/B = 5.5) for different parameters are calculated from FE analysis. The numerical results obtained from FE analysis are compared with the experimental ultimate load per unit area values of Sethy et al. [12] and are given in Table 2. The FE results appear to be in good agreement with those obtained by Sethy et al. [12]. The deviations between experimental and FE results are within 13%.

Proc. of the Eighth Intl. Conf. on Advances in Civil, Structural and Mechanical Engineering - CSM 2019

ISBN: 978-1-63248-170-2 DOI : 10.15224/978-1-63248-170-2-15

Table 2 Comparison of $q_{u\,(H/B,\,e/B)}$ from FE analysis with experimental values of Sethy et al. [12]

H/B	α/ϕ	e/B	$q_{u\,(H/B,\,e/B)}$ (kN/m^2)		Deviation (%)
			Sethy et al. [12]	HSM	
0.3	0	0	880	800	9.09
0.3	0	0.05	810	760	6.17
0.3	0	0.10	690	630	8.70
0.3	0	0.15	565	500	11.50
0.5	0	0	425	410	3.53
0.5	0	0.05	390	360	7.69
0.5	0	0.10	330	310	6.06
0.5	0	0.15	270	250	7.41
1	0	0	194	176	9.28
1	0	0.05	170	148	12.94
1	0	0.10	144	128	11.11
1	0	0.15	110	96	12.73
2	0	0	128	117	8.59
2	0	0.05	120	110	8.33
2	0	0.10	104	100	3.85
2	0	0.15	92	91	1.09
3	0	0	119	110	7.56
3	0	0.05	111	100	9.91
3	0	0.10	94	86	8.51
3	0	0.15	83	74	10.84
5.5	0	0	116	110	5.17
5.5	0	0.05	104	100	3.85
5.5	0	0.10	88	86	2.27
5.5	0	0.15	77	76	1.30

Distinctive plots of eccentric load per unit area of the footing $q_{(H/B,\,e/B)}$ vs. average settlement (s) with varying H/B ratio at a particular e/B = 0.05 are shown in Fig. 3. In both the laboratory model tests by Sethy et al. [12] and finite element analysis, all the parameters are kept constant except the thickness of sand layer (H). The behavior of the footing on sand layer with the rigid rough base at a great depth (H/B = 5.5) from laboratory model tests and FE analysis is also shown in Fig. 3 for comparison purpose. Fig. 3 shows that the ultimate eccentric load per unit area increases from 104 kN/m^2 to 810 kN/m^2 (rigid base at great depth i.e H/B = 5.5) in laboratory model tests and from 100 kN/m^2 to 760 kN/m^2 (H/B = 0.3) by FE analysis. When the rigid base is at a very shallow depth (H/B = 0.3 below the footing base) the ultimate load per unit area is increased up to about 7.5 times. For the same (H/B) ratio, the rigid base at limited depth improves the performance of the footing by increasing the ultimate eccentric load per unit area and reducing the settlement. From the Fig. 3, it can be seen that the load-displacement curve obtained from laboratory model tests by Sethy et al. [12] and FE analysis are of a similar pattern.

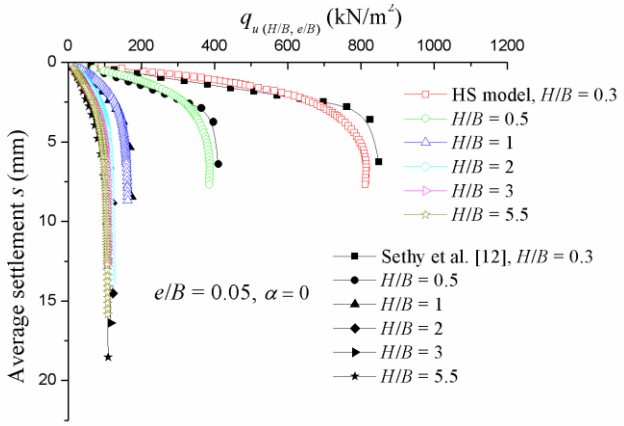

Figure 3. Variation of load-settlement plot with H/B for Model tests and FEM

B. *Effect of Rigid Base on the Foundation*

The ultimate eccentric load per unit area values $q_{u\,(H/B,\,e/B)}$ obtained from FE analysis are close to those obtained from the laboratory model tests by Sethy et al. [12] (Fig. 4). The general trends of the variation $q_{u\,(H/B,\,e/B)}$ with H/B ratio agree fairly well in both laboratory model tests and FE analysis. Fig. 4 shows the variation of $q_{u\,(H/B,\,e/B)}$ with H/B for e/B = 0, 0.05, 0.10, and 0.15. It may be seen from these plots that, for different e/B, the ultimate eccentric load per unit area decreases and reaches a minimum value at around H/B' = 3 (B' =B-2e) for both laboratory model tests and FE analysis.

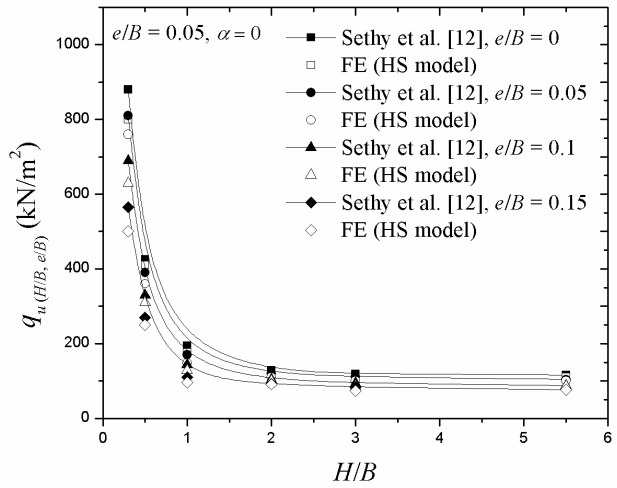

Figure 4. Variation of $q_{u\,(H/B,\,e/B)}$ with H/B

C. *Variation of N_γ^* for Vertical Centric Loading*

For numerical model with vertical and centric loading conditions (α/ϕ = 0, e/B = 0) in Table 2, the modified bearing capacity factor, N_γ^* can be obtained as

$$N_\gamma^* = \frac{q_{u\,(H/B,\,\alpha/\phi=0,\,e/B=0)}}{0.5\gamma B\lambda_\gamma^*} \qquad (1)$$

Proc. of the Eighth Intl. Conf. on Advances in Civil, Structural and Mechanical Engineering - CSM 2019

ISBN: 978-1-63248-170-2 DOI : 10.15224/978-1-63248-170-2-15

Using the $q_{u\,(H/B,\,\alpha/\phi=0,\,e/B=0)}$ values shown in Table 12 and modified shape factor, $\lambda_{\gamma}^{*} = 0.6$ as suggested by Cerato and Lutenegger [13], the variation of N_{γ}^{*} with *H*/*B* have been determined and shown in Fig. 5 along with the laboratory model test results provided by Cerato and Lutenegger [13] and Sethy et al. [12]. The agreement appears to be good.

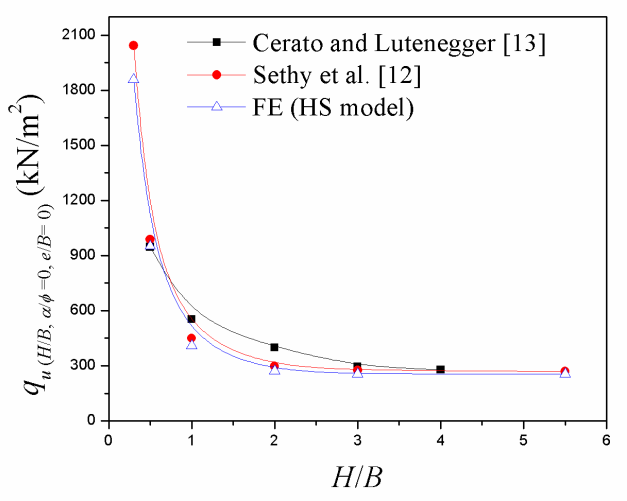

Figure 5.Variation of modified bearing capacity factor N_{γ}^{*} with *H*/*B*

D. *Failure Mechanism*

An incremental displacement at failure for vertical (*e*/*B* = 0, and $\alpha = 0$) and eccentric loading (*e*/*B* > 0) with rigid base at a great depth (*H*/*B* =5.5) is shown in Figs. 6, 7, and 8. Incremental displacement is the observation of deformations within the soil mass when a failure occurs. From Fig. 6, it is seen that the failure surface with the rigid base at a great depth is symmetrical on both sides and similar to the failure mechanism given by Terzaghi [15] under vertical loading. An elastic wedge zone is located immediately below the footing which pushes away the soil in two symmetrical zones (combination of radial shear zone and passive wedge zone). In contrast, under eccentric loading condition, an asymmetrical failure surface prevails [Fig. 7]. The larger the load eccentricity, smaller the failure surface is, and, consequently, smaller the ultimate load. Fig. 8 shows the extent of failure surface decreases with increasing the values of *e*/*B*.

The failure mechanism and their major failure surface comparison of circular foundation with rigid base at a limited depth (*H*/*B* small) are presented in Figs. 9 through 12. Figs. 9 through 12 show the development of failure surfaces in sand below the footing under vertical loading when analyzed FE analysis. For footings with rigid rough basements, namely *H*/*B* < *H*/*B*′, the rigid rough basement has a significant effect on their failure mechanisms. The extent of the failure surfaces in horizontal direction decrease with decreasing *H*/*B* ratio and the vertical extent is confined at the sand-basement interface.

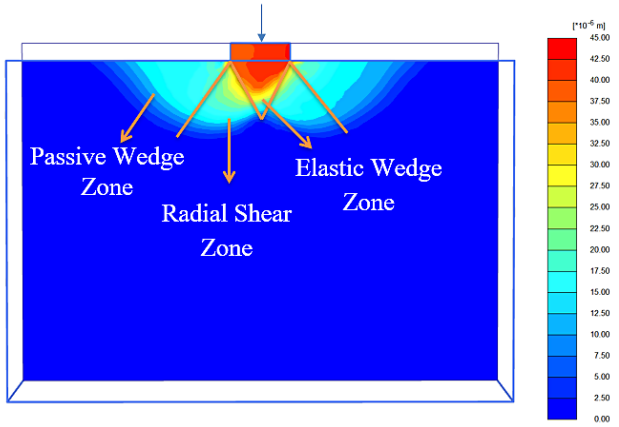

Figure 6. Incremental displacement in terms of relative shadings (*H*/*B* = 5.5, *e*/*B* = 0)

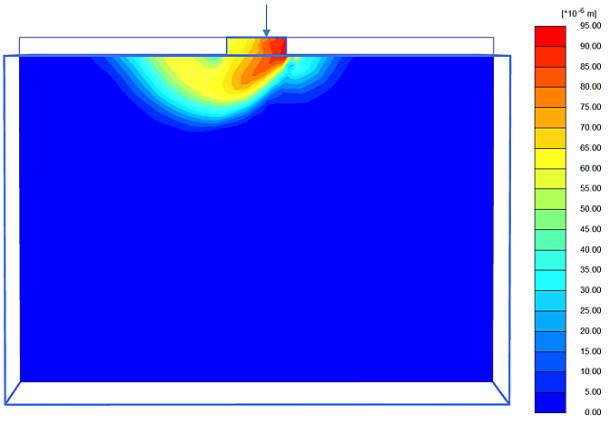

Figure 7. Incremental displacement in terms of relative shadings (*H*/*B* = 5.5, *e*/*B* = 0.05)

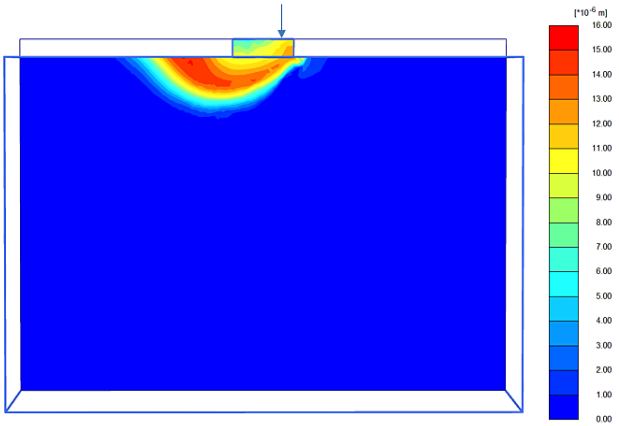

Figure 8. Incremental displacement in terms of relative shadings (*H*/*B* = 5.5, *e*/*B* = 0.15)

Proc. of the Eighth Intl. Conf. on Advances in Civil, Structural and Mechanical Engineering - CSM 2019

ISBN: 978-1-63248-170-2 DOI : 10.15224/978-1-63248-170-2-15

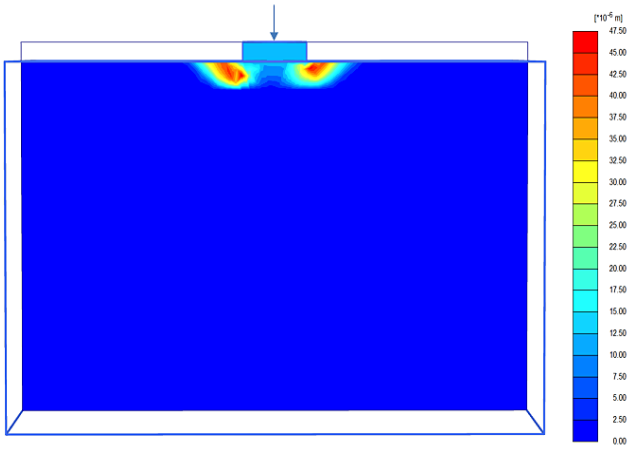

Figure 9. Incremental displacement in terms of relative shadings (H/B = 0.3, e/B = 0)

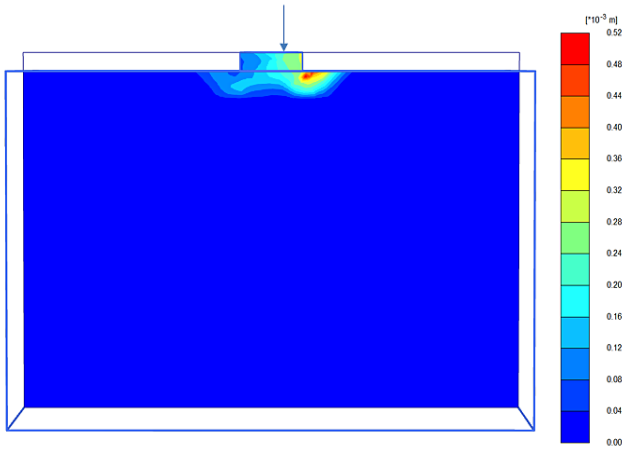

Figure 10. Incremental displacement in terms of relative shadings (H/B = 0.3, e/B = 0.05)

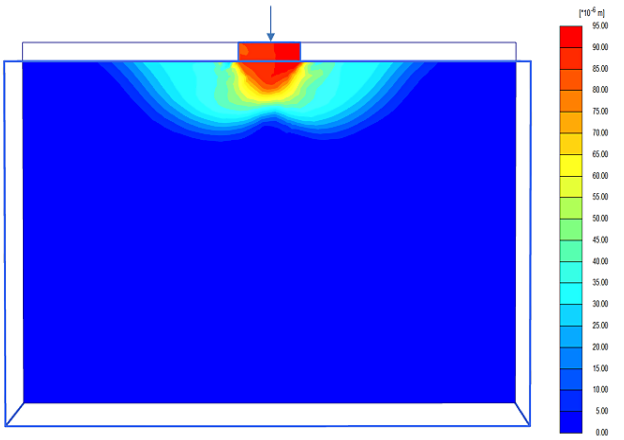

Figure 11. Incremental displacement in terms of relative shadings (H/B = 3, e/B = 0)

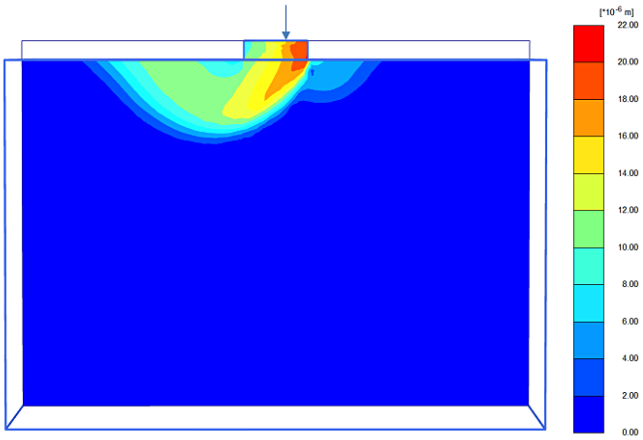

Figure 12. Incremental displacement in terms of relative shadings (H/B = 3, e/B = 0.05)

v. Conclusions

A numerical study of the behavior of eccentrically loaded circular footing over a sand layer of limited thickness is presented. Based on this study the following conclusions can be drawn

i. The ultimate bearing capacity values obtained from the FE analysis using HS model are presented. The comparison between HS model values and the experimental values of Sethy et al. [12] shows a good agreement and the deviation are within 13%.

ii. As revealed from the numerical model, the ultimate eccentric load per unit area $q_{u\ (H/B,\ e/B)}$ increases with a decrease in the depth of the rigid base. The ultimate eccentric load per unit area is dependent on H/B ratio and it becomes constant beyond $H/B' = 3$ (where, $B'=B-2e$), for all load eccentricity.

iii. Modified bearing capacity factor N_γ^* becomes constant at $H/B' \geq$ about 3 (where, $B' = B - 2e$) for all load eccentricities. The FE results appears to be in well agreement with the laboratory model test results of Sethy et al. [12] and Cerato and Lutenegger [13]

iv. It is observed that the failure mechanism is symmetrical on both sides of the footing under vertical load whereas under an eccentric load the failure mechanism is uneven.

v. The width of the failure surface in horizontal direction increases with increase in H/B ratio. Similarly, the vertical extent of the failure surface is confined at the sand-rigid base interface. The extent of failure surface decreases with increase in load eccentricity.

References

[1] Boushehrian, A.H., Hataf, N., Ghahramani, A., "Modeling of the cyclic behavior of shallow foundations resting on geomesh and grid-anchor reinforced sand." Geotext. Geomem. Vol. 29, 2011, pp. 242–248.

[2] Laman, M., Yildiz, A., "Numerical studies of ring foundations on geogrid- reinforced sand." Geosynth. Int. Vol. 14, 2007, pp. 52–64.

ISBN: 978-1-63248-170-2 DOI : 10.15224/978-1-63248-170-2-15

[3] Loukidis, D., Salgado, R., "Bearing capacity of strip and circular footings in sand using finite elements." Comput. Geotech. Vol. 36, 2009, pp. 871–879.

[4] Ornek, M., Demir, A., Yildiz, A., Laman, M., "Numerical analysis of circular footings on natural clay stabilized with a granular fill." Acta. Geotech. Slov. Vol. 9, 2012, pp. 61–75.

[5] Kaya, N., Ornek, M., "Experimental and numerical studies of T-shaped footings." In: Acta Geotech. slov., 2013, pp. 43–58.

[6] Demir, A., Yildiz, A., Laman, M., Ornek, M., "Experimental and numerical analyses of circular footing on geogrid-reinforced granular fill underlain by soft clay." Acta Geotech. Vol. 9, 2014, pp. 711–723.

[7] Baars S. Van., "The bearing capacity of footings on cohesionless soils. Electron." J. Geotech. Eng., Vol. 20, 2015, pp.12945–12955.

[8] Yang, F., Zheng, X.C., Zhao, L.H., Tan, Y.G., "Ultimate bearing capacity of strip footing placed on sand with a rigid basement." Comput. Geotech. Vol. 77, 2016, pp. 115-119.

[9] Brinkgreve, R.B.J., Vermeer, P., "Finite element code for soil and rock analysis." A. A. Balkeme, Rotterdam, Netherlands, 1998.

[10] Schanz, T., Vermeer, P.A., "Special issue on pre-failure defomation behaviour of geomaterials." Géotechnique, Vol. 48, 1998, pp. 383-387.

[11] Vesic, A.S., "Analysis of ultimate loads of shallow foundations. J. Soil. Mech. Found. Div., Vol. 99, 1973, pp. 45–73.

[12] Sethy, B.P., Patra, C.R., Das, B.M., Sobhan, K., "Bearing Capacity of Circular Foundation on Sand Layer of Limited Thickness Underlain by Rigid Rough Base Subjected to Eccentrically Inclined Load." Geotech. Testing J. ASTM, 2018, https://doi.org/10.1520/GTJ20170420

[13] Cerato, A.B., Lutenegger, A.J., "Bearing Capacity of Square and Circular Footings on a Finite Layer of Granular Soil Underlain by a Rigid Base." J. Geotech. Geoenv. Eng. Vol. 132, 2006. pp. 1496–1501.

[14] Terzaghi, K., "Theoretical Soil Mechanics. John Wiley & Sons, Inc., Hoboken, NJ, USA, 1943.